Effect of Squeezing Conditions on the Particle Distribution and B ond Line Thickness of Particle Filled Polymeric Thermal Interface Materials

Mahmood, R.S. Shirazy[1], Stéphanie Allard[2], Martin Beaumier[2], Luc, G. Fréchette[1]
[1]Department of Mechanical engineering, Université de Sherbrooke, QC, Canada, J1K 2R1
[2]IBM Corp., Bromont, QC, Canada
Reza.shirazy@usherbrooke.ca

ABSTRACT

An experimental study is performed to characterize the effect of squeezing conditions on the particle distribution and bond line thickness of particle filled polymeric thermal interface materials (TIM). Two different commercial particle-filled polymeric TIMs with different particle volume fractions have been used in this study. Rheological properties such as yield stress and viscosity are measured experimentally. Using laser granulometry technique, particle sizes have been measured and are further confirmed by SEM imaging. The TIM is then deposited on circular copper samples and is squeezed with different pressing rates. Analyzing the samples by acoustic microscopy technique shows that at low pressing rates the particle distribution is not uniform and a TIM branching phenomena can be observed. At higher pressing rates, the final thickness of the bond line is approximately 30% higher than low velocity pressing rates. By keeping the load on the sample at the end of the pressing procedure the final BLT will continue to decrease. It can be concluded that the optimum condition of TIM dispense procedure should include a high velocity pressing rate to attain a uniform particle distribution followed by a constant load period to obtain the minimum BLT.

KEY WORDS: Particle filled polymer, thermal interface material (TIM), bond line thickness (BLT), Assembly process

NOMENCLATURE

BLT	Bond line thickness, m
c	Constant = 13708
D	Substrate diameter, m
d	Particle diameter, m
h	Gap thickness, m
F	Squeezing force, N
K	Consistency index
n	Power law index
P	Squeezing pressure, Pa
R	Thermal resistance, C/W
Greek symbols	
γ	strain
η	Viscosity, Pa.s
τ	Shear stress, Pa
Subscripts	
c1 & c2	Contacting surfaces
interface	Interface between two solid surfaces
TIM	Thermal interface material
y	Yield

INTRODUCTION

The development of high performance microelectronics is becoming a key element in the today's world of science and technology. The challenge of coming up with higher performance devices is currently not only tied up to the electrical design of such devices, but also to the thermal management of the packaging system around them [1]. The need for more efficient thermal management solutions stems from the constant increase in the dissipating power in high end applications on one hand and the thinner and more compact form factors in consumer electronics, on the other hand. A well designed packaging solution should decrease the overall resistance in the thermal paths to alleviate the thermal constraint in the device performance.

One important source of the thermal resistance in the microelectronic packaging is the interface thermal resistance. In some packaging configurations, interface thermal resistance accounts for 50% of the overall thermal resistance [2]. It is known that when two solid surfaces are joined, asperities on each of the surfaces decrease the actual contact between the two solids to 1%-2% of the apparent area for lightly loaded interfaces [3]. The asperities are filled with air with very low thermal conductivity and pose a barrier in the thermal path between the two solid surfaces.

To alleviate the interface thermal resistance, thermal interface materials (TIMs) are used to fill the gaps and asperities between the two solids. Polymeric TIMs are one of the most widely used TIMs and are typically filled with highly thermally conductive particles (approximately 1-100 microns) to enhance their thermal conductivity [4]. The role of the particles is to conduct the heat between the two solid surfaces whereas the liquid matrix spreads on the surface. Particles are often chosen from high conductivity materials, such as metals (e.g. silver, copper) or ceramics (e.g. aluminum oxide, zinc oxide or boron nitride) and the matrix is a lower conductivity organic phase, such as silicone grease [5]. Volume fraction of the particles is chosen to be between 30%-80% [6]. Currently, effective thermal conductivity of the available commercial TIMs is on the order of 1-5 W/m K.

The overall thermal resistance across a TIM between two surfaces can be expressed through the following 1-D heat transfer model [4]:

$$R_{TIM} = R_{c1} + \frac{BLT}{k_{TIM} A_{interface}} + R_{c2} \qquad (1)$$

Where, R_{c1} and R_{c2} are the contact resistances of the two solid surfaces. The middle term shows the conductive thermal resistance of the TIM layer and is composed of bond line thickness (*BLT*), the TIM thermal conductivity, k_{TIM}, and the area of the interface, $A_{interface}$. To minimize this resistance, *BLT* should be minimized while TIM thermal conductivity and interface area should be maximized. Equation (1) shows that for accurately modeling the physics of the TIM performance,

three parameters including k_{TIM}, BLT and R_c should be understood.

Moreover, in order to apply a TIM on a surface, a number of assembly processes are required that may affect the final TIM properties. Dispensing, pressing and curing are generally required assembly steps for gel type polymeric TIMs [4]. It should be noted that except for the k_{TIM}, which is determined by the choice of materials and fabrication process used by the TIM manufacturer, BLT and R_c depend on the assembly process and surface materials. Furthermore, Post-process characterization has shown that, under certain conditions, the resultant bond lines formed between device and heat spreader may exhibit voids and may be non-uniform with respect to thickness and particle distribution. These anomalies may affect the thermal performance of the TIM over the life of a product, resulting in higher device operating temperatures and, in extreme cases, possible catastrophic failure of the device. Therefore, a good understanding of the impact of the assembly process on the final TIM properties is critical.

This work therefore aims to elucidate the effects of the assembly process on the TIM overall thermal resistance. The thermal resistance is characterized through the BLT and particle distribution and the impact of different pressing rates and conditions on these properties is studied experimentally.

GOVERNING EQUATIONS AND MODELS

Constitutive models for polymeric TIMs

Squeeze flows occur when a material is compressed between two parallel plates and thus squeezed out radially. In microelectronic packaging assemblies, TIMs are squeezed between the die and the heat spreader or heat sink [7]. Therefore, squeeze flow models can be used to find the behavior and the final BLT of the TIMs. In order to use the squeeze flow model including simplified mass and momentum conservations, an additional constitutive model is also required. This constitutive model should relate the shear stress experienced by the liquid to the strain rate. There are generally four types of constitutive models to describe the rheological behavior of the TIMs [8]. These models are Newtonian fluid, Power law fluid, Bingham fluid and Herschel-Bulkley (H-B) fluid. In a Newtonian fluid, viscosity is constant and does not depend on the strain rate [9]. Power law fluid is a Non-Newtonian fluid in which viscosity is not constant and depends on the shear rate. Viscoelastic fluids such as Bingham and H-B fluids additionally possess a yield stress after which they start to deform. Rheological tests on the TIMs show that they have a yield point and therefore, particle filled polymeric TIMs are Non-Newtonian and Viscoelastic fluids. Table 1 shows the constitutive equations and the final theoretical BLTs for these different fluids. An immediate observation in this table is that BLT is equal to zero for Newtonian and Power law models. This is clearly unrealistic for the particle filled polymeric TIMs because these materials possess well defined non-zero BLTs. Therefore, a starting point in the rheological study of the TIMs is to find if they behave like Bingham or H-B fluids.

BLT rheological modeling

Figure 1 shows the squeezing process of a thin layer of particle filled polymeric TIM between two circular plates. The BLT modeling can be done for two conditions: 1) constant radius of the TIM, i.e. the extra TIM flows out after squeezing; and 2) constant volume in which the squeezed TIM radius is smaller than the radius of the plates. In most real applications, the entire volume between the two components is not initially filled with the TIM, but will eventually reach the filled condition after starting the squeezing process. Therefore, condition 1 will be considered for the later discussions.

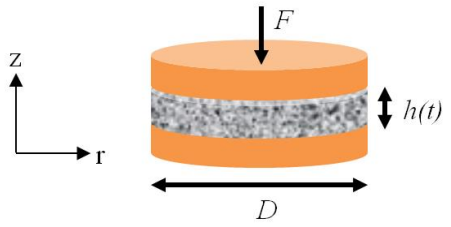

Figure 1 Schematic drawing of the TIM squeezing process

Some of the assumptions for the modeling of the BLT are [8]:

1) Lubrication assumption h << D is valid due to very small thickness of the TIM compared with the substrate diameter.
2) No slip boundary condition
3) Negligible inertial forces

Table 1 Constitutive equations and final BLT for different fluid models

Types of fluids	Constitutive equation (Viscosity)	Final BLT	Notes
Newtonian	$\eta = K$ & K=constant	BLT=0	η = viscosity
Power law	$\eta = K(\dot{\gamma})^{n-1}$ & K=constant	BLT=0	K = consistency index n = power law index $\dot{\gamma}$ = strain rate
Bingham	$\eta = \frac{\tau_y}{\dot{\gamma}} + K$ & K=constant	BLT=constant	τ_y = yield stress
Herschel-Bulkley (H-B)	$\eta = \frac{\tau_y}{\dot{\gamma}} + K(\dot{\gamma})^{n-1}$ & K=constant	BLT=constant	-

By measuring the viscosity of the various silicon-based particle filled polymeric TIMs, it is shown that these TIMs generally behave as H-B fluid [10, 11]. For the constant TIM radius and by defining the squeezing pressure as $P = F/\pi R^2$, the BLT will be:

$$BLT = \frac{2}{3} R \left(\frac{\tau_y}{P} \right) \tag{2}$$

where R is the radius of the circular disc and τ_y is the TIM yield stress. However, using Eq.2 for BLT will under predict the BLT by a large margin [12]. This is caused by assuming homogenous bulk properties in the very small length scales (in this case BLT) of the particle filled TIM [10]. At high squeezing pressures, the BLT thickness is comparable with the particle size and hence, the TIM becomes heterogeneous. Using finite size scaling of elasticity modules [4] for a thin percolating system, Prasher [12] suggests the so called scaling-bulk (S-C) model for BLT:

$$BLT = \frac{2}{3} R \left[c \left(\frac{d}{BLT} \right)^{4.3} + 1 \right] \left(\frac{\tau_y}{P} \right) \tag{3}$$

where c = 13708 and d is the particle diameter. Equation 3 reduces to Eq. 2 for small values of P/τ_y or when $BLT >> d$. Prasher [12] also proposes an approximate version of Eq. 3 for quick calculations:

$$BLT = \frac{2}{3} R \left(\frac{\tau_y}{P} \right) + \left(\frac{cR}{1.5} \right)^{0.188} d^{0.811} \times \left(\frac{\tau_y}{P} \right)^{0.188} \tag{4}$$

Particle distribution

When particle filled polymeric TIMs are dispensed over a surface, solid particles are assumed to be uniformly distributed in the matrix. In the assembly process, the TIM is squeezed between the two surfaces and a pressure driven flow is produced. Therefore, the initial volume fraction of the particles is altered in the remaining TIM between the two surfaces. Using Infrared microscopy to study the temperature distribution along the TIM vertical cross section [13], it has been shown that particle distribution can have significant effects on the thermal resistance of TIM. Two different phenomena; particle stacking and matrix filtration are related to the heterogeneous particle distribution and will be discussed in more detail in the following sections.

Particle stacking. As can be observed in Figure 2, during the squeezing, the TIM mixture tends to move to the sideways and away from the diagonals. The difference in flow lengths to the substrate edge leads to the flow paths with different pressure drop in the radial direction from the substrate center [14]. As the flow moves in the least resistance paths, the particles along the diagonal symmetry lines are pulled in opposite directions by the viscous matrix. Hence, they move with less velocity and are more likely to stack on each other. This phenomenon can increase the required squeezing force greatly and also affect the final thermal properties of the TIM through increased BLT and non-uniform thermal conductivity. Hierarchical channels are shown to provide paths for liquid flow and alleviate the particle stacking, both numerically and experimentally [2, 14, 15]. However, their application is still limited due to cost issues. It should be noted that in circular substrates the flow paths are equal from center to the edges and therefore, no stacking line is expected to be observed.

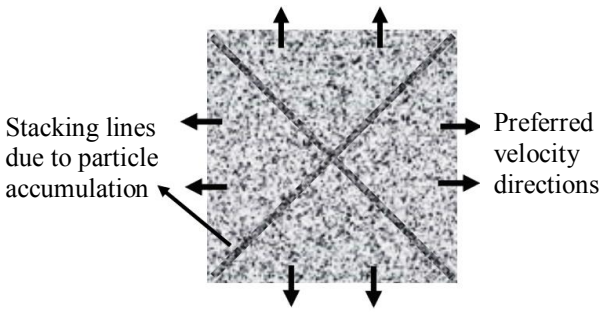

Figure 2 Diagonal stacking lines due to particle accumulation

Matrix filtration. When a highly particle filled polymer is squeezed very slowly, the particles may be entrapped and the base liquid can filter and flow relative to the particle network [16]. The filtration may greatly increase the squeezing force and the particle distribution homogeneity. Experimental results show that there is a critical squeezing velocity below which the filtration occurs. Above this velocity, the viscous forces are sufficient to carry the particles with the flow. Below this velocity, the viscous forces are not able to overcome the friction forces produced by the particle network, which tends to act as a porous media in this case. Due to the gradual increase of the polymer radial velocity towards the edges, the particle accumulation occurs first in the center region (low velocity region) [17].

EXPERIMENTAL METHODS

Materials

Two different commercial TIMs known as TIM A and TIM B were used in this study. These TIMs mainly consist of a silicon oil matrix and solid particles. These thermal interface materials contain other coupling agents and surfactants to enhance the wetting of the filler, increase the ultimate filler volume fraction and prevent the re-agglomeration of the fillers [10]. The precise value of the filler volume fraction was not known but it was generally between 30-75%. Some of the properties of these two TIMs can be seen in Table 2.

Table 2 Properties of the TIMs

TIM name	A	B
Bulk thermal conductivity (W/m K)	3.8	2.6
Density (kg/m^3)	2500	2400
Filler volume	Extremely high	High

Particle size analysis

The precise particle size distributions for these TIMs were not known. Therefore, laser granulometry technique was used to characterize the particle size distribution. In this technique,

a laser beam passes through a dispersed particulate sample and the intensity of the scattered light beam is then measured. This data is then analyzed to calculate the size of the particles that created the scattering pattern. A Mastersize 2000 (Malvern™) tool was used for laser granulometry. In this method, solid particles should be added to a dispersant. Therefore, solid particles should first be separated from the TIM polymer. The following method was used to separate the solid particles:

1. Dilute the TIM thoroughly with Hexane.
2. Use Centrifuge on 2500rpm for 10mins to separate the particles and wash out the silicon oil.
3. Carefully remove the transparent liquid (with no suspended particles) by a pipette. If the suspended particles are also removed, then the bigger size particles will not be detected.
4. Repeat step 3 and 4 to completely remove the silicon oil.
5. Let the samples to dry for 2 days.
6. Use a lab spoon to turn the samples into a fine powder

In order to make sure that no particle was discarded in step 3, the transparent liquid was left to dry on a clean glass surface and then the surface was examined with scanning electron microscope (SEM, S-4700 Hitachi) and no particles were observed. Therefore, it could be concluded that the analyzed powder contained all the solid particles in the TIM samples.

Rheological measurements

Dynamic and yield stress measurements were performed with a Viscotech rheometer (ATS RheoSystems) using parallel plate geometry (15mm) at constant temperature (25˚C). Dynamic measurements were carried out by varying the shear stress between 0.5 and 100 Pa while maintaining a constant frequency of 1 Hz. These measurements yielded the value of the storage shear modulus (G') in the linear viscoelastic region as well as the extent of this region. The yield stress values of the TIMs were determined via a stress-sweep experiment where the sample was sheared with decreasing stress values between 500 and 0.5 Pa. The yield stress value was determined as the stress where flow ceases or, in practice, as the peak viscosity attained in the downward stress sweep. Prior to measurement, all samples were pre-sheared to erase the rheological history of the sample.

BLT measurements

Circular copper samples with the diameter of 28mm were machined with a 31×31 mm rectangular base for the squeeze tests (Figure 3.a). The rectangular base size was chosen to fit in the standard sample holders already used for squeezing tests. The circular lids were also made of copper with a diameter of 28mm with 3mm thickness. The sample and lid were relatively thick to minimize the warpage effect. The upper surface of the sample and the lower surface of the lid were polished to decrease the roughness. An Infrared (IR) transparent plastic (0.38mm thickness) made by Edmund optics™ was used between the lid and the sample surface. The initial plan was to use a thermography approach to characterize the variation of temperature on the sample surface due to particle distribution in the TIM. However, the results were eventually not satisfying. In fact, the convection thermal resistance on the sample surface was several orders of magnitude higher than that of the conduction in the TIM, hence rendering the surface temperature variations undetectable. Samples were then placed in the sample holder and the IR transparent plastic is carefully placed on the TIM manually.

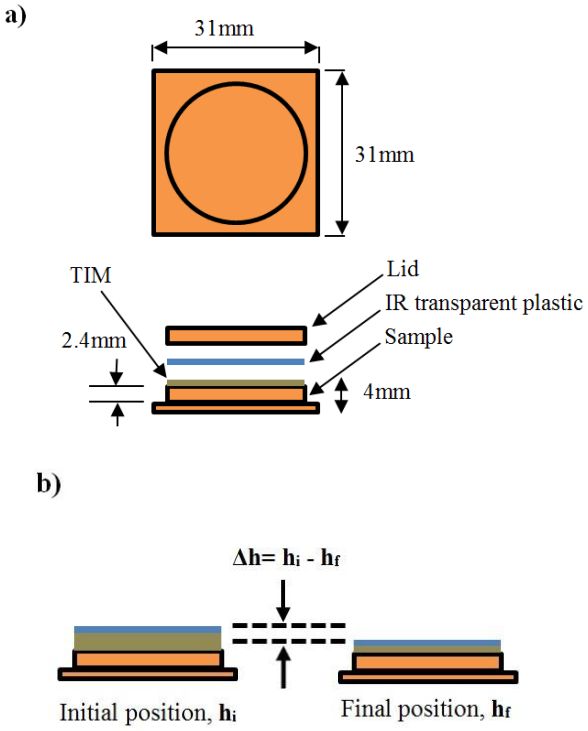

Figure 3 Schematic drawing of the sample-lid configuration and b) definition of the TIM relative displacement

A table top Instron™ (5900 series) mechanical testing machine was used for squeezing the samples. The squeezing head was equipped with a vacuum system that holds the lid before the squeezing tests. The squeezing tests could be performed either with constant rate of squeezing force or constant squeezing velocity until the prescribed final force is reached. Before each test, first the squeezing head and the attached lid were brought down until they were very close to the IR transparent plastic. Then the displacement sensor was set to zero and the test began. The machine lowered the lid with the prescribed squeezing rate until the force sensor measured 0.2N force due to touching the sample. Then the displacement and the force were measured in 0.01s intervals until reaching the final prescribed force. At the end of each test, the copper lid was removed and raised by the Instron™ machine but the IR transparent plastic remained on the sample surface.

The relative displacement of the TIM (Δh) was calculated by subtracting the initial position of the lid when touching the sample from the final position when the final prescribed force was reached (Figure 3.b). It should be noted that this is not the absolute TIM thickness. Using optical microscopy, the total height of the IR transparent plastic, the TIM and the circular part of the sample thickness were measured by focusing the image on the plastic and then on the sample sides. By subtracting the known values of the circular part of the sample

thickness and the IR plastic from the total measured thickness, the BLT could be obtained. At the final force, two cases were studied: either the lid position was held constant or the force was kept constant for 10s and the lid was left free to move.

The TIM was dispensed mechanically by a Camalot FX-D dispensing system from Speedline Technologies™ (Auger Pump dispense) with a star pattern on the sample surface (Figure 4). Using the standard TIM dispense procedure used by IBM, 0.215mg of TIM with 5% uncertainty was dispensed on the sample. This system ensured a very high precision and repeatable disperse TIM mass and pattern. Therefore, it was assumed that the initial TIM thickness was equal for all samples.

Figure 4 TIM dispense pattern on the copper sample

Following squeezing process, the samples were examined with acoustic microscopy. The acoustic microscope (Sonoscan GEN5) was equipped with a 50 MHz transducer and operated in Front Interface Echo (FIE) mode. It was focused at the first interface between the IR transparent plastic and the TIM layer. It was therefore possible to observe variations in the structure by monitoring how much acoustic energy was reflected back to the transducer versus that transmitted through the interface into the bond line volume.

RESULTS AND DISCUSSIONS

TIM rheological parameters

Rheological measurements were performed on the two TIM types: TIM A and TIM B. The yield stress of the two TIMs can be seen in Figure 5 .a. As stated before, the yield stress is defined as the point where the maximum viscosity is obtained Figure 5.b shows the non-linear dependency between the viscosity and strain rate. It can be seen that the experimental data can be best modeled by the H-B model. Therefore, these TIMs behave as the H-B model. From the measured yield stresses of the TIMs and by fitting the experimental data of viscosity vs. strain rate with the H-B constitutive model, the unknown constants in this model can be found. These values are shown in Table 3.

Table 3 H-B parameters of the TIMs

TIM name	A	B
Yield stress (Pa), τ_y	100	14
K	607	418
n	0.266	0.437

It can be seen that the yield stress of the TIM A is more than the TIM B. It can be attributed to the higher amount of particle volume fraction seen in Table 2. This is consistent with other experimental results for particle filled polymeric TIMs [10, 12].

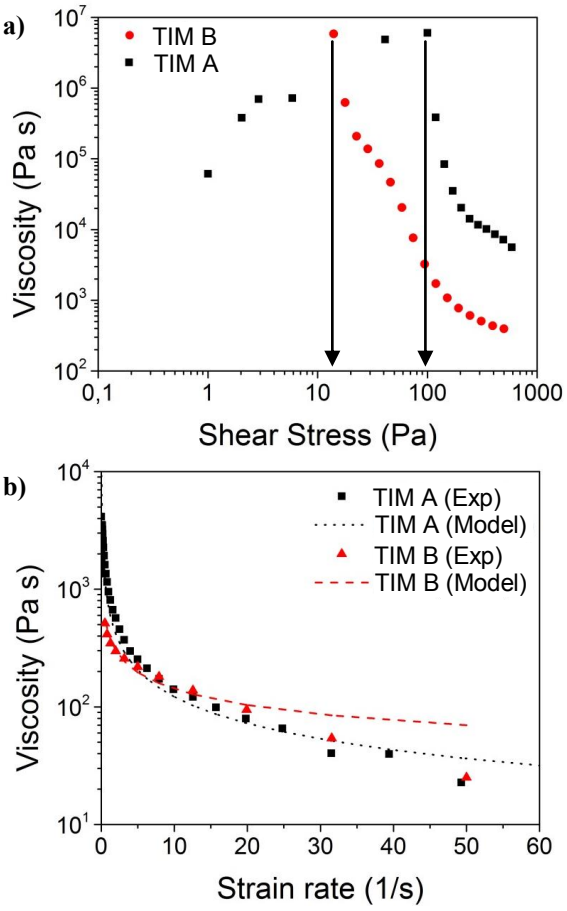

Figure 5 .a) Viscosity versus shear stress to determine yield stress b) experimental and theoretical results from H-B model for viscosity versus strain rate for two different TIM types

Particle size distributions

Figure 6 shows the particle size distribution obtained by Laser granulometry method. It can be seen that the particle diameter sizes are similar with two peaks at 1.5µm and 13µm which can be attributed to two different particle types. However, the volume fraction of the bigger particles is higher for the TIM A. It should be noted that this measured volume fraction is not the real TIM volume fraction because it only shows the ratio of the particles with respect to the dispersed base liquid in the laser granulometry device and not the TIM. Figure 7 shows a SEM image of the separated particles of the TIMs. It is important to note that although the apparent measured smaller particle size is around 1.5µm but the SEM image shows an agglomeration of these particles. Agglomeration of nanoparticles is due to adhesion of particles to each other by weak forces leading to (sub) micron-size entities [18]. Therefore, the real diameter of these particles is less than 1.5µm shown by laser granulometry method.

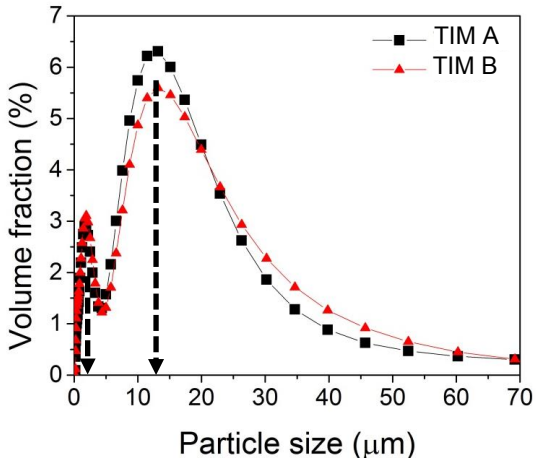

Figure 6 Particle size distributions for the two TIM types

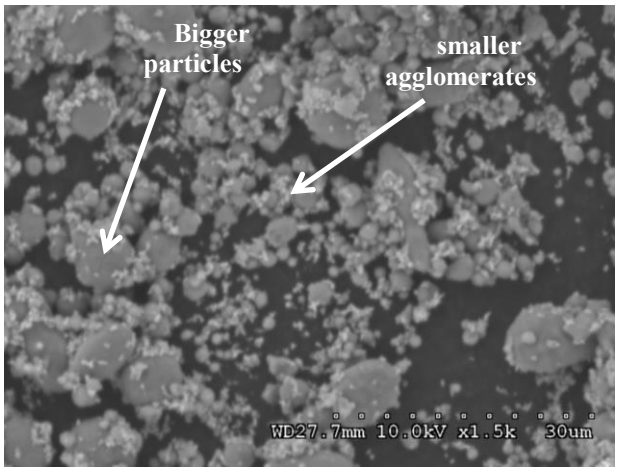

Figure 7 SEM image of the particles extracted from the TIM. Two different particle types can be identified.

Effect of squeezing rate on the TIM thickness

Effect of squeezing rate on the BLT and the particle distribution was investigated by varying the TIM pressing rate. Only one of the TIMs (TIM A) was selected for the squeezing tests. Three different constant squeezing force rates were used to investigate the TIM behavior. A constant force squeezing rate was applied and the displacement was measured. The final force was set to 110N which was within the range of force used on real packaging products. Figure 8 shows the results of the relative TIM thickness versus the squeezing force for three different squeezing force rates. The lid position is held constant at the end of the test. It can be observed that after an initial large deformation with a relatively low squeezing force, the deformation rate decreases. The initial large deformation is caused by the small surface area between the TIM and the lid before complete spreading of the TIM. After the TIM has spread over most of the surface, the deformation decreases due to higher viscous forces. Although the initial TIM thickness and sample dimensions are equal for the three cases, the relative TIM displacements (Δh) are not equal. Higher squeezing rates result in smaller TIM displacements (Δh) which in practice will lead to higher BLTs.

This behavior can be explained by the Maxwell model for viscoelastic materials [19]. Viscoelastic materials have the properties of both viscous and elastic materials. When the deformation rate is high (rapid motion in short times) the viscoelastic material tends to react as a solid and the resulting shear stress increases significantly. This can be better viewed in Figure 9 where the lid velocity is depicted as a function of time. It can be seen that there is a sharp peak at higher squeezing rates which is followed by a decrease in the lid velocity. This sharp peak is not observed in the lower squeezing rates.

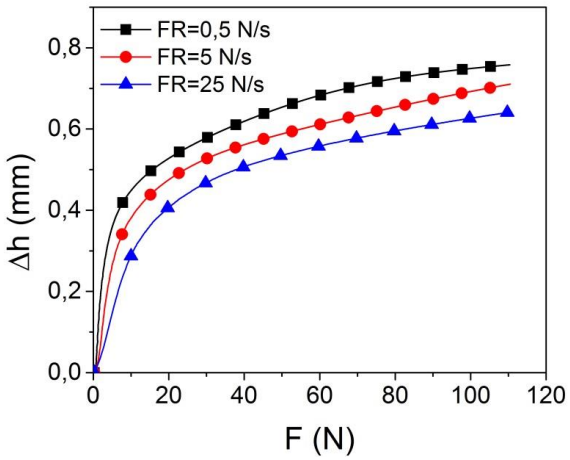

Figure 8 Variation of the relative TIM thickness versus the squeezing force

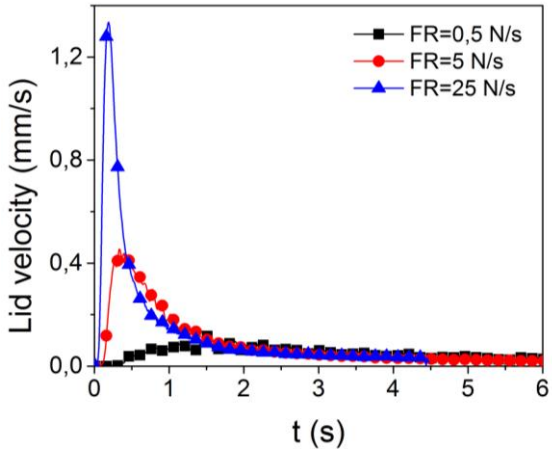

Figure 9 Lid velocity as a function of time

Figure 10 shows the relative displacement of the TIMs when the final force (F=110N) is kept constant for 10s and the lid is left free to displace. It can be seen that in both Figure 10.a and b, the TIM keeps deforming after reaching the final force. Comparing Figure 10.a and b shows that the variation of TIM relative height (Δh) once the force reaches F=110N is smaller at high squeezing rate of 25 N/s (Figure 10.b). However, the final TIM relative displacement (Δh) after 10s is almost the same for both high and low squeezing rates and will eventually be identical if given enough time. These results show that the relative TIM deformation does not depend on the squeezing rate if the final force is kept constant for a

certain amount of time. Therefore, the final BLT is obtained by keeping the squeezing force constant.

It is interesting to note that the TIM deformation during the constant force 10s period is higher for the high squeezing rate compared with the lower squeezing rate (Figure 10.a). The percentage of relative TIM displacement with respect to its position after reaching F=110N and after 10s is summarized in Table 4. It can be seen that for high values of squeezing rate, the TIM thickness continues to decrease up to 10% of its initial height.

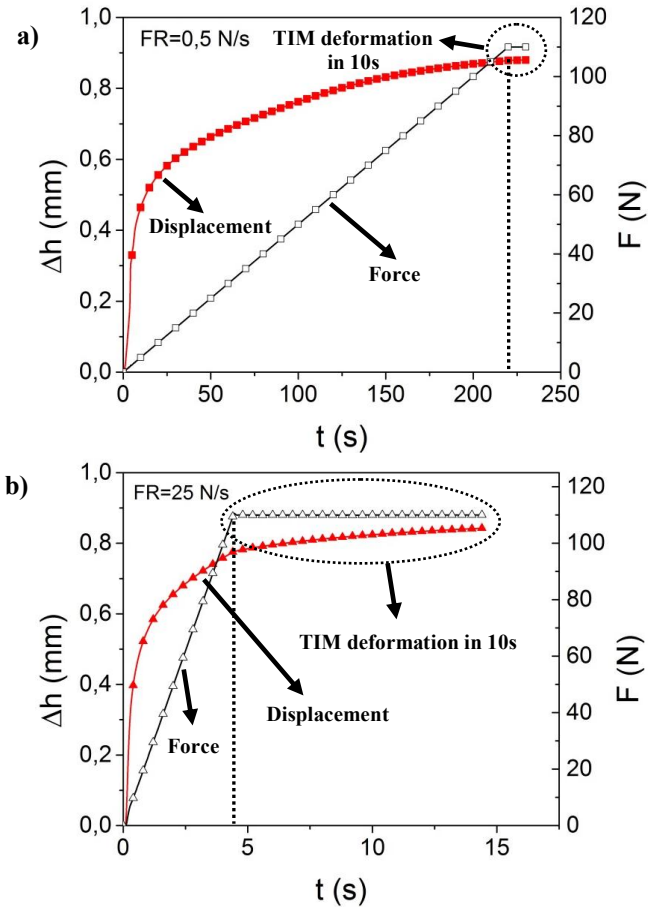

Figure 10 Relative TIM thickness variation after reaching the final force of F=110 N and keeping this force for 10s

Table 4 Values of relative TIM deformation after reaching the final force

Squeezing rate (N/s)	% of relative deformation with respect to the thickness at F=110N
0.5	0.1
5	5
25	9

Figure 11 shows the measured values of BLT and the theoretical values obtained by S-C model (Eq. 3). The theoretical values are calculated by using particle diameter of d = 13μm, c = 13708 (obtained by Prasher [12]) and τ_y = 100 Pa. It can be seen that the experimental results are slightly lower than the theoretical model results. To obtain the experimental value from the S-C model, the constant c should be around 50 which is significantly different from the 13708 presented in [12]. It should be noted that the value of c = 13708 presented in [12] is found for single particle size TIM and not a bimodal TIM like the present study. This may explain the difference in the values of c.

The experimental uncertainties in Figure 11 are significant especially for the high force (F=110N). This is mainly due to the uncertainties caused by the copper sample dimensions and the BLT measurement method (optical microscopy). This shows that the BLT should be studied with more accurate samples and measurement methods.

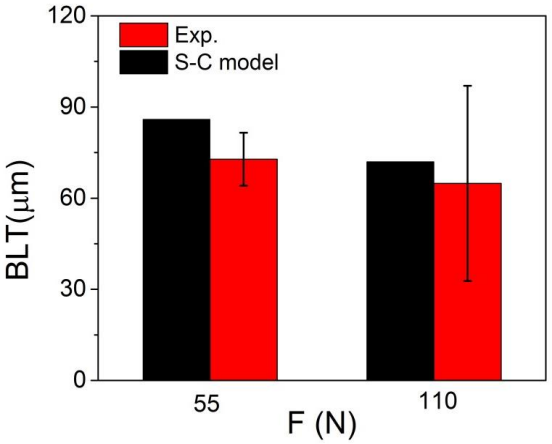

Figure 11 Experimental and theoretical values of the BLT

Effect of squeezing rate on the particle distribution

Figure 12 shows the effect of different squeezing rates on the particle distribution obtained by acoustic microscopy. The dark regions at the sample edges are caused by the TIM overflow during squeezing. As the squeezing rate increases from 0.5 N/s to 25 N/s, the particle distribution on the TIM surface becomes more uniform and no more segregation can be observed. The uniform TIM distribution caused by the high squeezing rate (Figure 12.c) may be explained by the Maxwell theory for viscoelastic materials [19]. At high squeezing rates, the TIM deformation rate is so high that the material behaves more like elastic solid and not like a liquid. Therefore, it deforms with isotropic properties including the particle distribution. As the squeezing rate decreases the fluid nature of the material becomes more dominant and the particles tend to segregate from the matrix.

Based on the matrix filtration phenomena, the particle concentration should be more in the center region and less towards the edges. However, Figure 12.a and b show and opposite trend which is unexpected. This unexpected behavior may be caused by the surface quality of the copper samples or the TIM wetting properties on the copper. Although not shown here, IBM internal tests performed on silicon chips have demonstrated this effect with the expected pattern (particle concentration higher at the center region).

Optimum TIM assembly process

An optimum thermal contact by a TIM should have the least thermal resistance which can be achieved by using a high thermal conductivity material and a low BLT.

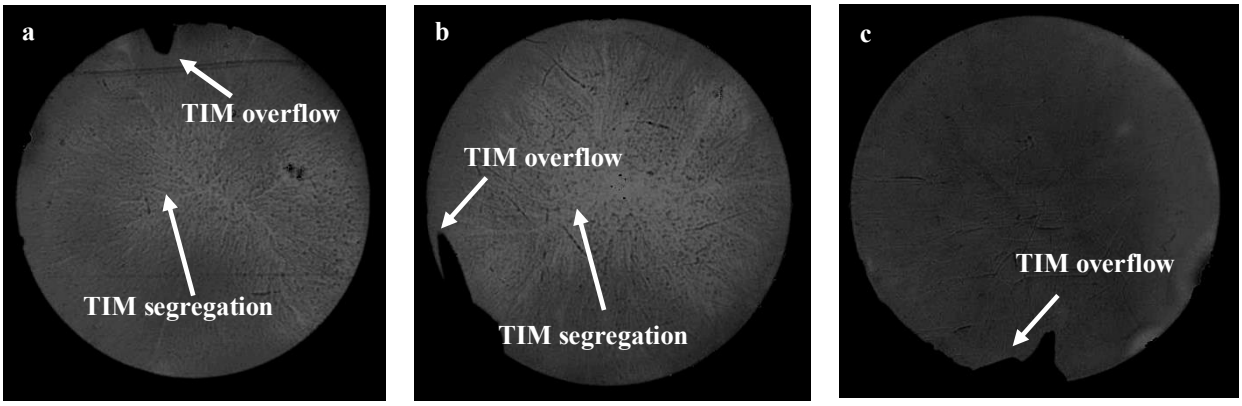

Figure 12 Images of the acoustic microscopy for different squeezing rates of a) 0.5 N/s b)5 N/s and c) 25 N/s

Uniform particle distribution is also important as it may affect the final BLT through stacking phenomena or variation in the local thermal conductivity due to the variable particle concentration. Because the TIM bulk thermal conductivity is determined by the TIM vendor, it is not affected by the assembly process. Therefore minimum BLT and a uniform particle distribution are the main objectives of an optimum assembly process. The previous results show that this optimum condition may be obtained by first squeezing the TIM with a high squeezing rate and then holding the force until the final minimum BLT is achieved. In this way, both minimum thermal resistance and uniform particle distribution is obtained.

CONCLUSIONS

Particle filed polymeric thermal interface materials (TIMs) are studied by theoretical and experimental approaches. Thermal conductivity, thermal contact resistance, bond line thickness (BLT) and particle distribution are identified as the important factors related to their thermal performance. Among these factors, bond line thickness (BLT) and particle distribution are determined by the assembly process and therefore an experimental approach is used to explore them in more depth. Two common commercial TIMs, are used in the experimental part of this study and the following conclusions can be drawn:

1- As the knowledge of the TIMs microstructure is critical in all the modeling efforts, experimental approaches are used to characterize the TIMs. A method to separate the solid particles from the liquid matrix is devised and then the particle size distributions are obtained by the laser granulometry method. Two particle sizes are detected in the TIMs and the results are further confirmed by SEM images.
2- Rheological properties of the TIMs are important to determine the type of fluid model. These properties are measured experimentally and the fluid model is identified as Herschel-Bulkley (H-B). The yield stress and the constants for the two TIMs are also determined experimentally.
3- The final BLT is calculated by the scaling-bulk (S-C) model and the results are in good agreement with the experimental values. However, the experimental uncertainties due to sample dimensions and BLT measurement method are significant.
4- The effect of squeezing rate on the relative TIM thickness is investigated experimentally. It is observed that by increasing the squeezing rate, the thickness of the TIM increases which can be justified by the Maxwell theory. However, by keeping the constant load on the TIM, the thickness will continue to decrease and eventually a certain final BLT is reached for all squeezing rates.
5- The acoustic microscopy results show that the particle distribution will be uniform in the high squeezing rates. This shows that the optimum assembly process may include a fast squeezing process flowed by a period of constant load on the electronic component to achieve the smallest BLT.

ACKNOWLEDEGMENTS

This research was funded by the ENGAGE program of NSERC and in kind contributions of IBM Canada. Financial support was also provided by the Canada Research Chair program for personnel and NanoQuébec for infrastructures at the Université de Sherbrooke.

REFRENCES

[1] Tong, X.C., 2011, "advanced materials for thermal management of electronic packaging," Springer, New York, pp. 616.

[2] Bajaj, N., Subbarayan, G., and Garimella, S. V., 2012, "Topological Design of Channels for Squeeze Flow Optimization of Thermal Interface Materials," International Journal of Heat and Mass Transfer, **55**(13-14) pp. 3560-3575.

[3] Prasher, R. S., 2001, "Surface Chemistry and Characteristics Based Model for the Thermal Contact Resistance of Fluidic Interstitial Thermal Interface Materials," Journal of Heat Transfer, **123**(5) pp. 969-975.

[4] Prasher, R., 2006, "Thermal Interface Materials: Historical Perspective, Status, and Future Directions," Proceedings of the IEEE, **94**(8) pp. 1571-86.

[5] Due, J., and Robinson, A. J., 2013, "Reliability of thermal interface materials: A review," Anonymous Elsevier Ltd, Langford Lane, Kidlington, Oxford, OX5 1GB, United Kingdom, **50,** pp. 455-463.

[6] Kanuparthi, S., Subbarayan, G., Siegmund, T., 2008, "An Efficient Network Model for Determining the Effective Thermal Conductivity of Particulate Thermal Interface Materials," IEEE Transactions on Components and Packaging Technologies, **31**(3) pp. 611-621.
[7] Khalsa, S., and Subbarayan, G., 2011, "Squeeze flow models for thermal interface materials contained between parallel plates and plates with posts," ASME 2011 Pacific Rim Technical Conference and Exhibition on Packaging and Integration of Electronic and Photonic Systems, InterPACK 2011, July 6, 2011 - July 8, OR, United states, **1,** pp. 263-269.
[8] Prasher, R. S., Shipley, J., Prstic, S., 2002, "Rheological study of micro particle laden polymeric thermal interface materials: Modeling (Part 2)," ASME 2002 International Mechanical Engineering Congress and Exposition, IMECE2002, November 17, 2002 - November 22, New Orleans, LA, United states, **7,** pp. 53-59.
[9] Engmann, J., Servais, C., and Burbidge, A. S., 2005, "Squeeze Flow Theory and Applications to Rheometry: A Review," Journal of Non-Newtonian Fluid Mechanics, **132**(1-3) pp. 1-27.
[10] Prasher, R. S., Shipley, J., Prstic, S., 2003, "Thermal Resistance of Particle Laden Polymeric Thermal Interface Materials," Journal of Heat Transfer, **125**(6) pp. 1170-1177.
[11] Prasher, R. S., Shipley, J., Prstic, S., 2002, "Rheological study of micro particle laden polymeric thermal interface materials: Experimental (Part 1)," ASME 2002 International Mechanical Engineering Congress and Exposition, IMECE2002, November 17, 2002 - November 22, New Orleans, LA, United states, **7,** pp. 47-51.
[12] Prasher, R. S., 2004, "Rheology based modeling and design of particle laden polymeric thermal interface materials," The Ninth Intersociety Conference on Thermal and Thermomechanical Phenomena In Electronic Systems, Piscataway, NJ, USA, **1,** pp. 36-44.
[13] Hu, X., Jiang, L., and Goodson, K. E., 2003, "Impact of wall region particle volume fraction distribution on thermal resistance of particle filled thermal interface materials [electronic packaging]," Nineteenth Annual IEEE Semiconductor Thermal Measurement and Management Symposium, Piscataway, NJ, USA, pp. 106-11.
[14] Linderman, R. J., Brunschwiler, T., Kloter, U., 2007, "Hierarchical nested surface channels for reduced particle stacking and low-resistance thermal interfaces," 23rd Annual IEEE Semiconductor Thermal Measurement and Management Symposium, SEMI-THERM, March 18, 2007 - March 22, San Jose, CA, United states, pp. 87-94.
[15] Brunschwiler, T., Kloter, U., Linderman, R. J., 2007, "Hierarchically Nested Channels for Fast Squeezing Interfaces with Reduced Thermal Resistance," IEEE Transactions on Components and Packaging Technologies, **30**(2) pp. 226-34.
[16] Delhaye, N., Poitou, A., and Chaouche, M., 2000, "Squeeze Flow of Highly Concentrated Suspensions of Spheres," Journal of Non-Newtonian Fluid Mechanics, **94**(1) pp. 67-74.
[17] Rae, D. F., Borgesen, P., and Cotts, E. J., 2011, "The Effect of Filler-Network Heterogeneity on Thermal Resistance of Polymeric Thermal Bondlines," JOM, **63**(10) pp. 78-84.
[18] Tyson, B. M., Abu Al-Rub, R. K., Yazdanbakhsh, A., 2011, "A Quantitative Method for Analyzing the Dispersion and Agglomeration of Nano-Particles in Composite Materials," Composites Part B: Engineering, **42**(6) pp. 1395-1403.
[19] Morrison, F.A., 2001, "Understanding Rheology," Oxford University Press, New York, pp. 560.